

High-Density Assembly of Gold Nanoparticles on Multiwalled Carbon Nanotubes Using 1-Pyrenemethylamine as Interlinker

Yen-Yu Ou and Michael H. Huang*

Department of Chemistry, National Tsing Hua University, Hsinchu 30013, Taiwan

Received: October 16, 2005; In Final Form: December 12, 2005

In this article, we describe the formation of carbon nanotube (CNT)–gold nanoparticle composites in aqueous solution using 1-pyrenemethylamine (Py–CH₂NH₂) as the interlinker. The alkylamine substituent of 1-pyrenemethylamine binds to a gold nanoparticle, while the pyrene chromophore is noncovalently attached to the sidewall of a carbon nanotube via π – π stacking interaction. Using this strategy, gold nanoparticles with diameters of 2–4 nm can be densely assembled on the sidewalls of multiwalled carbon nanotubes. The formation of functionalized gold nanoparticles and CNT–Au nanoparticle composites was followed by UV–vis absorption and luminescence spectroscopy. After functionalization of gold nanoparticles with 1-pyrenemethylamine, the distinct absorption vibronic structure of the pyrene chromophore was greatly perturbed and its absorbance value was decreased. There was also a corresponding red shift of the surface plasmon resonance (SPR) absorption band of the gold nanoparticles after surface modification from 508 to 556 nm due to interparticle plasmon coupling. Further reduction of the pyrene chromophore absorbance was observed upon formation of the CNT–Au nanoparticle composites. The photoluminescence of 1-pyrenemethylamine was largely quenched after attaching to gold nanoparticles; formation of the CNT–Au nanoparticle composites further lowered its emission intensity. The pyrene fluoroprobe also sensed a relatively nonpolar environment after its attachment to the nanotube surface. The present approach to forming high-density deposition of gold nanoparticles on the surface of multiwalled carbon nanotubes can be extended to other molecules with similar structures such as *N*-(1-naphthyl)ethylenediamine and phenethylamine, demonstrating the generality of this strategy for making CNT–Au nanostructure composites.

Introduction

Formation of carbon nanotube–metal nanoparticle composites enables the investigation of using such structures for heterogeneous catalysis and molecular sensing applications.¹ Various strategies have been adopted to attach metal nanoparticles onto the surface of carbon nanotubes. Covalent surface functionalization with carboxylic acid groups by treating carbon nanotubes with HNO₃ or H₂SO₄–HNO₃ mixture has been used to deposit Pt and Au nanoparticles.^{1–4} However, the chemical functionalization process is tedious if amine groups are desired for the deposition of gold nanoparticles, and the electronic properties of the carbon nanotubes may be changed.⁵ An extension of this strategy is the adsorption of cationic polyelectrolyte on the carboxylated surface of carbon nanotubes and the attachment of negatively charged gold nanoparticles to the polyelectrolyte chains through electrostatic interactions.^{6,7} Wrapping of non-functionalized carbon nanotubes with negatively charged polystyrene sulfonate, followed by the adsorption of cationic polyelectrolyte poly(diallyldimethylammonium chloride) has also been used to assemble gold nanoparticles and nanorods.^{8,9} Yet, coating of carbon nanotubes with a thick polymer layer may block the electron transport pathway if electrode junctions using gold nanorods and molecular sensing through attached nanoparticles were considered.¹⁰

In contrast to the above surface functionalization and polymer wrapping approaches, attachment of metal nanoparticles to

carbon nanotubes using interlinkers such as pyrene derivatives which interact with carbon nanotubes via π – π stacking represents a simple and attractive strategy. The intrinsic electronic properties of the carbon nanotubes are preserved, and surface functional groups on the nanotubes can be easily varied by changing the pyrene derivatives. Using this procedure, proteins,¹¹ polyelectrolyte layers,¹² DNA strands linked to gold nanoparticles,¹³ and magnetic nanoparticles¹⁴ have been successfully assembled onto the sidewalls of carbon nanotubes. Gold nanoparticle assembly on carbon nanotubes using thiol-terminated pyrene interlinkers has also been demonstrated.¹⁵ However, pyrene derivatives with alkylamine groups have not been used to attach gold nanoparticles to carbon nanotubes. Furthermore, changes in the optical spectra over the entire particle deposition process have in general not been thoroughly monitored.

In this article, we examine the assembly of gold nanoparticles on the surface of multiwalled carbon nanotubes using 1-pyrenemethylamine (Py–CH₂NH₂) as the interlinker. Binding of Py–CH₂NH₂ to gold nanoparticles in a toluene–THF mixture and the corresponding optical changes have been investigated.¹⁶ The extent of nanoparticle coverage was inspected with electron microscopy. Absorption and emission changes at several stages of the CNT–Au nanoparticle composite formation process were monitored, as spectroscopic characterization of the process is more convenient than microscopy, and more physical insights can be provided. Finally, we tested the generality of this nanocomposite formation approach by using phenethylamine and *N*-(1-naphthyl)ethylenediamine as interlinkers to show that

* To whom correspondence should be addressed. E-mail: hyhuang@mx.nthu.edu.tw.

molecules with mono- and polycyclic aromatic structures can also assemble gold nanoparticles densely on carbon nanotubes.

Experimental Section

Synthesis of Multiwalled Carbon Nanotubes. Silicon wafers cut to 1 cm \times 1 cm were first boiled with piranha acid ($\text{H}_2\text{SO}_4/\text{H}_2\text{O}_2$ in 4:1 volume ratio) for 45 min and stored in deionized water. These wafers with a native oxide layer were sputtered with a 5-nm iron thin film as catalyst. To synthesize carbon nanotubes, the wafers were placed in the middle of a 1-in quartz tube. The tube was purged with 95 sccm of argon for 20 min, and then, the furnace temperature was raised to 750 $^\circ\text{C}$ in 20 min. At this point, 5% acetylene in argon atmosphere was introduced as the carbon source. The flow rates of acetylene and argon were 5 and 95 sccm, respectively. After reaction for 30 min, acetylene flow was stopped, and the furnace was allowed to cool in argon atmosphere to collect the carbon nanotubes.

Preparation of Gold Nanoparticles. Gold nanoparticles were prepared using a previously described procedure for making gold seeds with sizes of 2–4 nm.¹⁷ A volume of 0.2 mL of 0.025 M sodium citrate solution was added to 19.8 mL of aqueous solution containing 2.5×10^{-4} M HAuCl_4 and stirred for 3 min. Concurrently, 10 mL of 0.01 M NaBH_4 solution was prepared by adding NaBH_4 to 10 mL of ice-cold 0.025 M sodium citrate solution. When 0.6 mL of the NaBH_4 solution was added to the HAuCl_4 solution, the resulting solution immediately turned orange-red, indicating the formation of gold nanoparticles. All reagents were obtained from Aldrich.

Formation of CNT–Au Nanoparticle Composites. To 4 mL of the gold nanoparticle solution was added 10 μL of 0.5 N NaOH to make the solution pH slightly more basic; protonation of $\text{Py}-\text{CH}_2\text{NH}_2$ forming $-\text{NH}_3^+$ cations is thus avoided. However, the solution pH remained acidic at 5–6. Then, 100 μL of 10^{-3} M 1-pyrenemethylamine hydrochloride (95%, purchased from Aldrich) in ethanol was added to the gold nanoparticle solution and stirred for 30 min. The concentration of 1-pyrenemethylamine hydrochloride in the resulting solution was 24 μM . UV–vis absorption and photoluminescence spectra of the solution were taken. Next, 1 mg of the synthesized carbon nanotube sample was added to the solution and stirred for 6 h. The resulting solution was grayish purple in color and was then analyzed and stored in a refrigerator.

Two other compounds were also used as interlinkers for the formation of CNT–Au nanoparticle composites. A 5-mL aliquot of 2.5×10^{-3} M *N*-(1-naphthyl)ethylenediamine dihydrochloride ($\text{C}_{10}\text{H}_7\text{NHCH}_2\text{CH}_2\text{NH}_2 \cdot 2\text{HCl}$, 98%, purchased from Aldrich) aqueous solution was added to 0.5 mL of the gold nanoparticle solution and stirred for 12 h. Next, 5.5 mL of the resulting solution was mixed with 0.75 mL aqueous solution of the synthesized carbon nanotubes (0.1–0.3 mg carbon nanotubes) and stirred for 18 h. Similarly, 5 mL of 2.5×10^{-3} M phenethylamine sulfate ($(\text{C}_6\text{H}_5\text{CH}_2\text{CH}_2\text{NH}_2)_2 \cdot \text{H}_2\text{SO}_4$, 97%, purchased from Aldrich) aqueous solution was added to 0.5 mL of the gold nanoparticle solution and stirred for 12 h. Then, 5.5 mL of the resulting solution was mixed with 0.75 mL aqueous solution of the synthesized carbon nanotubes (0.1–0.3 mg carbon nanotubes) and stirred for 18 h. These reaction conditions, which are somewhat different from those used for the 1-pyrenemethylamine interlinker, were adopted to minimize particle aggregation, and no NaOH was added to the gold nanoparticle solution. A low 1-pyrenemethylamine concentration in the gold nanoparticle solution is necessary to prevent excimer formation, which may interfere with the optical characterization.

Instrumentation. Scanning electron microscopy (SEM, JEOL JSM-6330F) was employed to examine the synthesized carbon nanotubes on substrates. Raman spectra were obtained using a Triax 550 spectrometer with an excitation wavelength of 632.8 nm from a He–Ne laser to reveal the crystallinity of the nanotubes. UV–vis absorption spectra were taken on a JASCO V-570 spectrophotometer. Photoluminescence spectra were recorded using a Jobin-Yvon-Fluorolog-3 spectrofluorometer. Transmission electron microscopy (TEM, JEOL JEM2010 and TECNAI 20, both operated at 200 kV) was used for the examination of the synthesized carbon nanotubes and the CNT–Au nanoparticle composites.

Results and Discussion

This study attempts to prepare a high-density assembly of gold nanoparticles on the surface of carbon nanotubes using mono- and polycyclic aromatic compounds with alkylamine groups as interlinkers. Figure 1 gives the schematic illustration of the strategy used to assemble gold nanoparticles on the surface of carbon nanotubes. In this case, gold nanoparticles are surface-modified with 1-pyrenemethylamine. The alkylamine group can bind to a gold nanoparticle through the lone pair of electrons on the nitrogen atom.¹⁶ These modified gold nanoparticles can subsequently assemble on the surface of carbon nanotubes via π – π stacking interactions between the pyrene portion of the molecule and carbon nanotubes.

Figure 2a shows a SEM image of the multiwalled carbon nanotubes synthesized in this study for the formation of CNT–Au nanoparticle composites. Dense arrays of vertically grown carbon nanotubes were formed over the entire substrate surface. A close examination of these nanotubes shows that they are twisted and can often be entangled with neighboring nanotubes as they continue their upward growth (see Figure 2b). The synthesized carbon nanotubes can reach uniform lengths of over 50 μm , with diameters ranging between 30 and 100 nm. The Raman spectrum of the as-synthesized carbon nanotubes is displayed in Figure 2c. It reveals two bands centered at 1317 cm^{-1} (D band) and 1567 cm^{-1} (G band), which are characteristic Raman features for carbon nanotubes. The value of I_D/I_G , a measure of the degree of crystallinity of carbon nanotubes, is ~ 0.72 . This value indicates that the as-synthesized carbon nanotubes possess a relatively high degree of structural perfection, considering that the reaction temperature is just 750 $^\circ\text{C}$.¹⁸

Figure 3a shows a TEM image of the CNT–Au nanoparticle composites using 1-pyrenemethylamine as the interlinker. A magnified view of the lower portion of Figure 3a is provided in Figure 3b. A high-magnification TEM image of the nanocomposites showing the graphitic sheets of multiwalled carbon nanotubes is available in Supporting Information Figure 1, although a different sample was imaged. Gold nanoparticles with mainly diameters of 2–4 nm are uniformly attached over the surface of carbon nanotubes without fusion into larger particles. Direct addition of Au nanoparticles to carbon nanotubes was also tested as a control; only few nanoparticles were observed on the surface of carbon nanotubes in this case. The abundant presence of immobilized gold nanoparticles on the carbon nanotubes, compared to an insignificant amount of nanoparticle coating in the control experiment, demonstrates that 1-pyrenemethylamine can effectively assemble gold nanoparticles on the surface of carbon nanotubes. The energy-dispersive X-ray spectrum (EDS) of the CNT–Au nanoparticle composites is presented in Figure 3c. Carbon and gold signals are detected, confirming the attachment of gold nanoparticles onto carbon nanotubes.

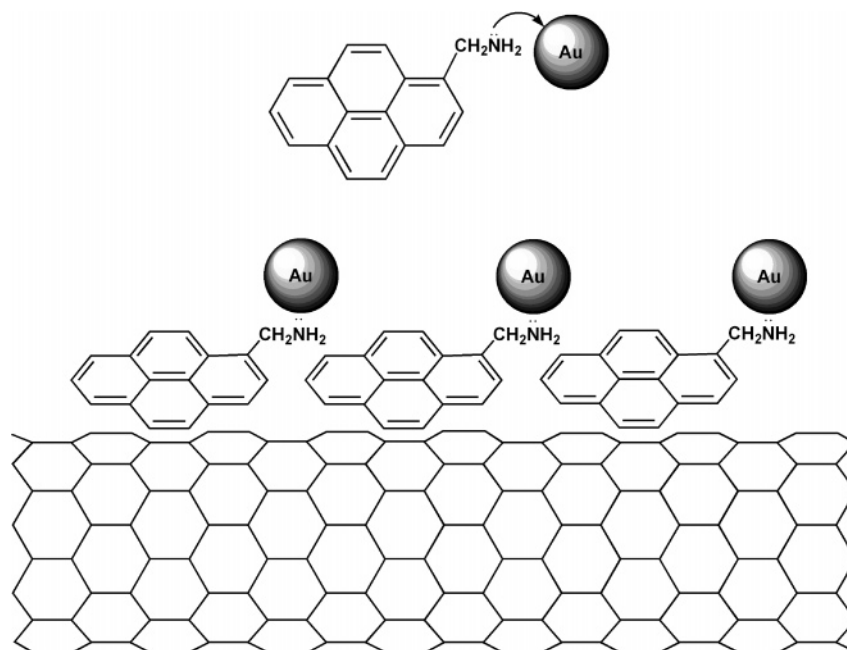


Figure 1. A schematic illustration of gold nanoparticle assembly on carbon nanotubes through 1-pyrenemethylamine interlinker.

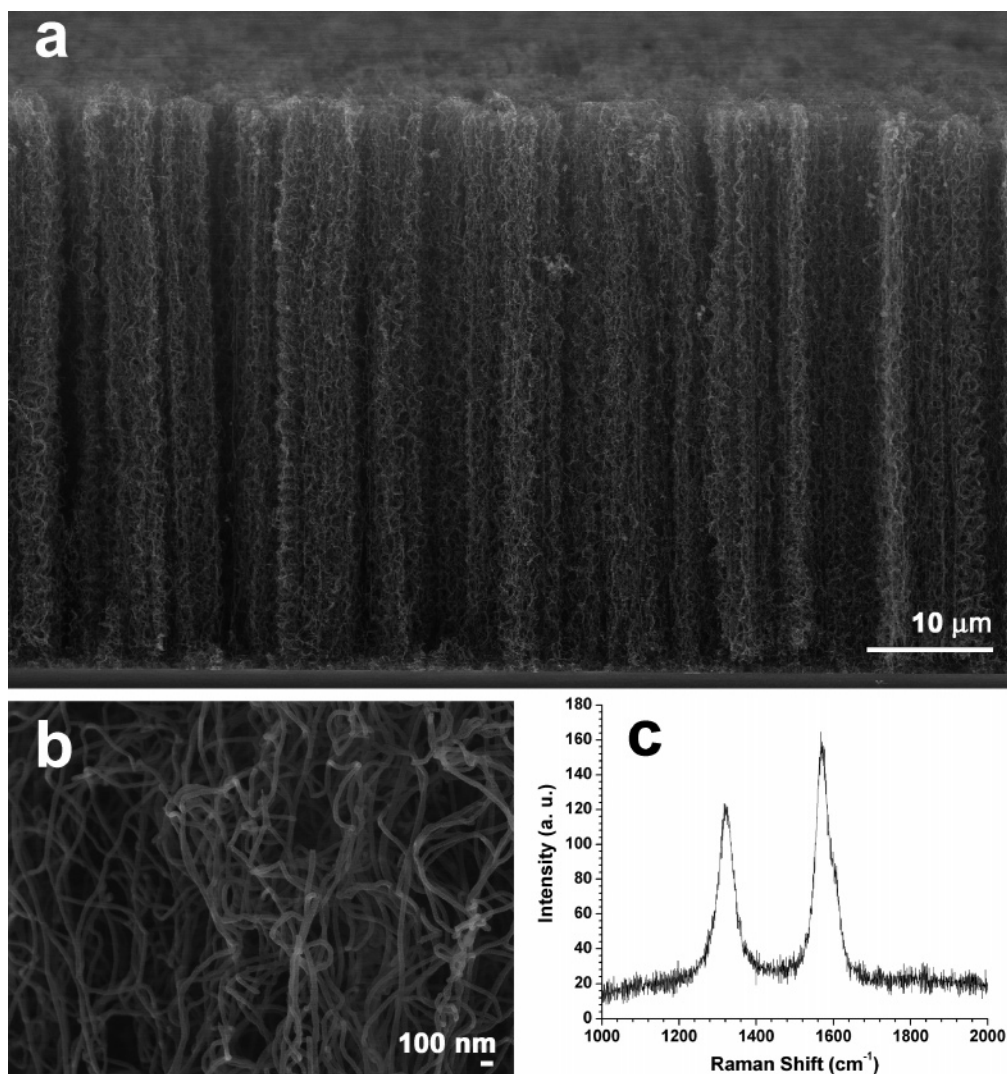


Figure 2. (a) SEM image of the synthesized vertically grown carbon nanotubes. (b) A high-magnification SEM image of the synthesized carbon nanotubes. (c) Raman spectrum of the synthesized carbon nanotubes.

In addition to verifying the formation of CNT–Au nanoparticle composites with TEM characterization, UV–vis absorption

and photoluminescence spectroscopy have been used to provide further insights into the optical changes at various stages of the

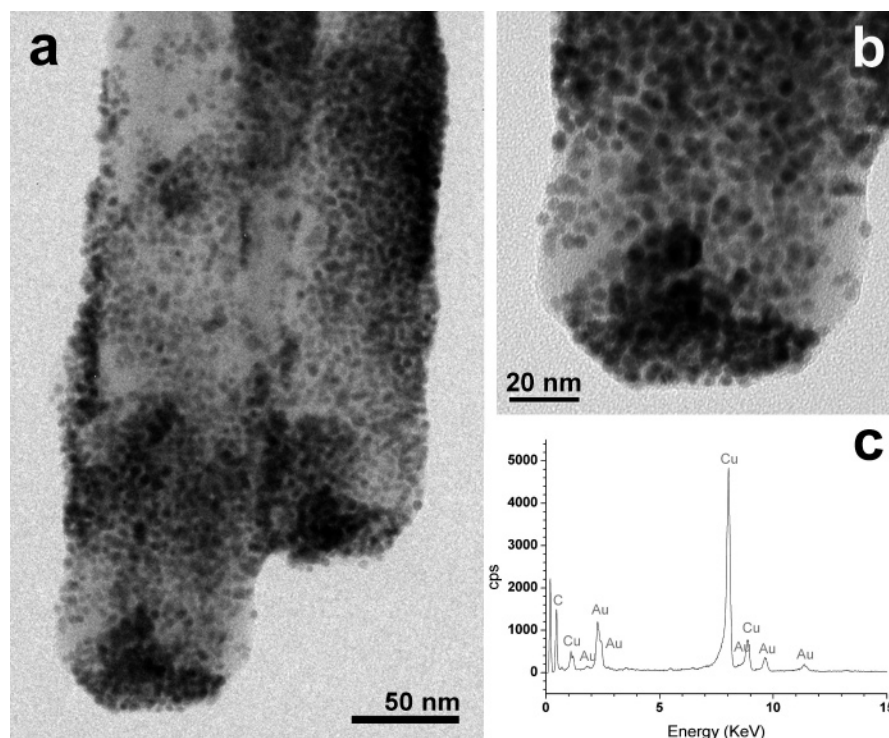


Figure 3. (a) TEM image of the CNT–Au nanoparticle composites. (b) A high-magnification TEM image of the lower portion of panel (a) showing high-density deposition of individual Au nanoparticles. (c) EDS spectrum of the CNT–Au nanoparticle composites. The copper signals come from the copper TEM grid.

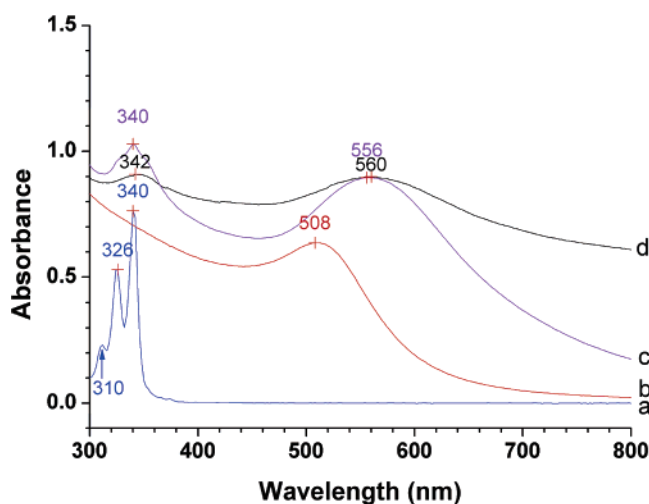


Figure 4. UV–vis absorption spectra of (a) free 1-pyrenemethylamine in ethanol, (b) aqueous gold nanoparticle solution, (c) the mixture of 1-pyrenemethylamine and gold nanoparticles, and (d) the solution containing CNT–Au nanoparticle composites.

nanocomposite formation process. The UV–vis absorption spectrum of free 1-pyrenemethylamine in ethanol reveals three major vibronic bands at 310, 326, and 340 nm (trace a, Figure 4). The as-synthesized gold nanoparticles with diameters of 2–4 nm exhibit a surface plasmon resonance (SPR) absorption band centered at 508 nm (trace b, Figure 4). No or little change in the absorption maximum was observed with the small amount of NaOH added. Upon attachment of 1-pyrenemethylamine to gold nanoparticles in water, the sharp and distinct vibronic structures of the molecules were no longer well resolved and with considerably lower absorbance values (trace c, Figure 4). This perturbation of the structured absorption bands of 1-pyrenemethylamine reflects changes in its electronic properties upon its complexation to a gold nanoparticle, which arises from a

strong ground-state interaction between the plasmon electrons of gold nanoparticles and the π -electron cloud of pyrene chromophore.¹⁹ Surface functionalization of gold nanoparticles with 1-pyrenemethylamine also red-shifts the SPR absorption band of the gold nanoparticles to 556 nm (trace c, Figure 4). The red shift of the SPR band is attributed to interparticle plasmon coupling, a phenomenon observed even when just a few gold nanoparticles or nanorods are clustered together.^{20,21} The result suggests that some of these surface-modified gold nanoparticles are in close proximity with each other but are not agglomerated, as evidenced by the TEM images of the CNT–Au nanoparticle composites. The reduction in the overall surface charge of the gold nanoparticles after binding to 1-pyrenemethylamine may have caused some nanoparticles to come close together. Finally, when the functionalized gold nanoparticles were attached to carbon nanotubes, the absorption vibronic feature of 1-pyrenemethylamine was essentially lost as a result of the π – π interactions between the pyrenyl group of 1-pyrenemethylamine and the sidewalls of the carbon nanotubes (trace d, Figure 4). The position of the broad SPR absorption band stayed almost unchanged with a band maximum at 560 nm. The absorbance values for all wavelengths of this sample increased greatly; carbon nanotubes are black, so they absorb all wavelengths of visible light. The results suggest that the functionalized gold nanoparticles have been successfully attached to carbon nanotubes, and no further aggregation of the gold nanoparticles occurred on the surface of carbon nanotubes.

The fluorescence of 1-pyrenemethylamine showed significant quenching upon interactions with gold nanoparticles and carbon nanotubes. Monomeric 1-pyrenemethylamine in ethanol exhibits strong vibronic emission with distinct peaks at 376, 386, and 396 nm, as shown in the inset of Figure 5. Its emission was largely quenched after binding to gold nanoparticles (trace a, Figure 5) and further but moderately quenched after the formation of CNT–Au nanoparticle composites (trace b,

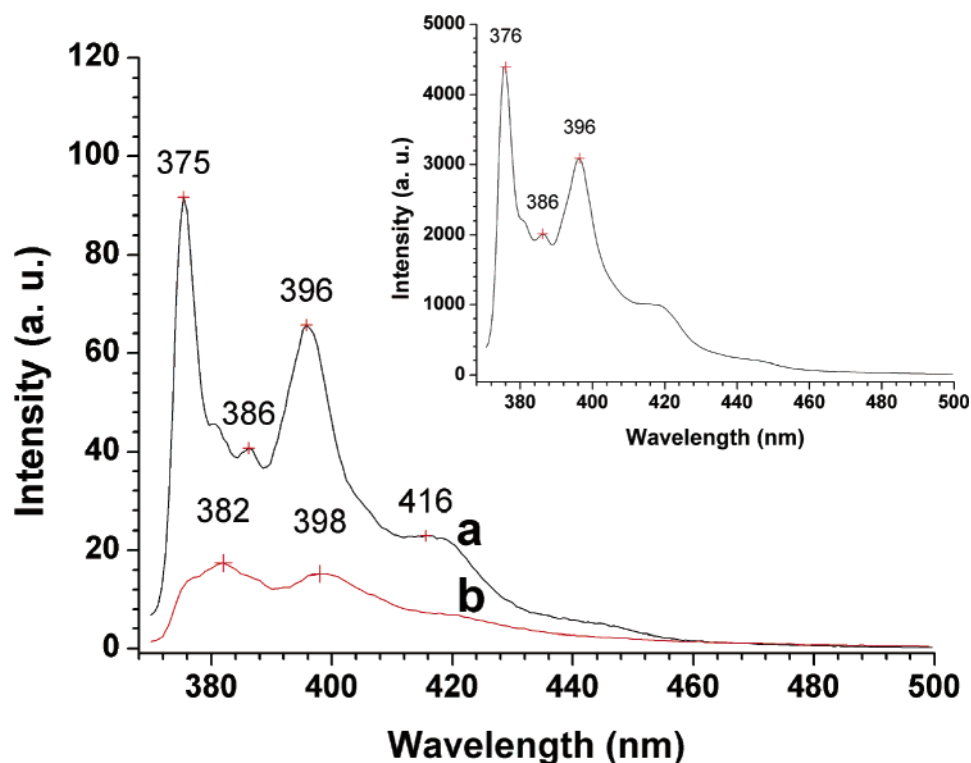


Figure 5. Photoluminescence spectra of (a) 1-pyrenemethylamine in the Au nanoparticle solution and (b) 1-pyrenemethylamine after forming the CNT–Au nanoparticle composites. Inset shows the photoluminescence spectrum of 1-pyrenemethylamine in ethanol with a concentration of 24 μ M. Excitation wavelength used was 341 nm.

Figure 5). The vibronic structure of its fluorescence after binding to gold nanoparticles is similar to that of the unbound 1-pyrenemethylamine but with noticeably lower intensity; the maintenance of its spectral feature is due to similar polar environment of the fluoroprobe. The relative peak intensities in the emission spectrum of 1-pyrenemethylamine after the formation of CNT–Au nanoparticle composites have changed markedly, a sign of the change of the fluoroprobe surroundings to a more nonpolar environment (that is, the nonpolar surface of carbon nanotubes). This sensitivity of the luminescence characteristics of 1-pyrenemethylamine to the polarity of its environment is similar to that of pyrene, with the intensity ratio of band III to band I increasing to a larger value from a polar to a nonpolar environment.²² The band III/I ratio, where band I is the peak at 376 nm and band III at 386 nm, increases from 0.43 for 1-pyrenemethylamine bound to gold nanoparticles in aqueous solution to ~ 1.25 after the formation of CNT–Au nanoparticle composites. The fluorescence results show that the decay of singlet excited 1-pyrenemethylamine is strongly affected by its binding to gold nanoparticles as well as carbon nanotubes. The drastic decrease in the fluorescence intensity of 1-pyrenemethylamine upon binding to gold nanoparticles indicates that a large fraction of the excited fluoroprobe was quenched by gold nanoparticles as a result of energy transfer²³ or electron transfer^{16,19,24} from 1-pyrenemethylamine to the gold nanoparticles. Both processes are considered to be the major deactivation pathways for excited fluoroprobes on a metal surface. Similar nonradiative decay processes may have caused further luminescence quenching of 1-pyrenemethylamine after the formation of CNT–Au nanoparticle composites via the π – π stacking interactions between the pyrene chromophore and the carbon nanotubes.

The strategy of using 1-pyrenemethylamine as the interlinker to form high-density arrays of gold nanoparticles on the

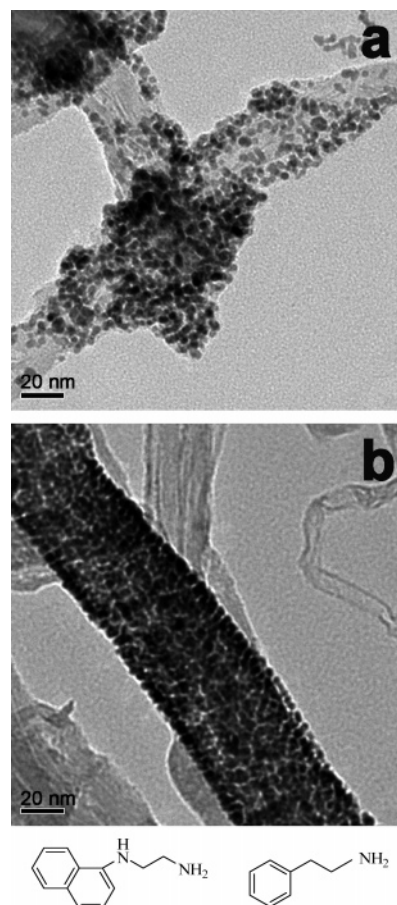


Figure 6. High-magnification TEM images of CNT–Au nanoparticle composites using (a) *N*-(1-naphthyl)ethylenediamine and (b) phenethylamine as interlinkers.

sidewalls of carbon nanotubes can be extended to other molecules with similar structures. It is conceivable that molecules containing mono- and polycyclic aromatic structures and alkylamine substituents can also serve as effective interlinkers. Figure 6 shows the high-resolution TEM images of CNT–Au nanoparticle composites using *N*-(1-naphthyl)ethylenediamine and phenethylamine as interlinkers. Again, high-density deposition of gold nanoparticles 2–4 nm in diameter on the surface of carbon nanotubes was observed in both samples. Although only high-resolution TEM images are shown here, many other carbon nanotubes examined also showed substantial coverage with gold nanoparticles. The results demonstrate that the strategy used in this study to densely assemble gold nanoparticles on the sidewalls of carbon nanotubes is generally applicable to other molecules with similar structures and functionalities.

Conclusion

High-density assembly of gold nanoparticles on the sidewalls of multiwalled carbon nanotubes using 1-pyrenemethylamine as the interlinker has been demonstrated. The alkylamine substituent of the pyrene derivative binds to a gold nanoparticle, while the pyrene fluorophore is in contact with the sidewall of a carbon nanotube via π – π stacking interaction. These functionalized gold nanoparticles with diameters of 2–4 nm are uniformly dispersed over the surface of carbon nanotubes. The formation process of the CNT–Au nanoparticle composites was monitored by UV–vis absorption and photoluminescence spectroscopy. A large absorbance decrease and perturbation of the absorption vibronic structure of the pyrene derivative were observed upon its binding to gold nanoparticles and carbon nanotubes. There was also a corresponding red shift of the SPR band of the gold nanoparticles, which is attributed to interparticle plasmon coupling of some nanoparticles in close contact with one another. Significant quenching of the luminescence of 1-pyrenemethylamine upon binding to gold nanoparticles was recorded, as a result of energy transfer or electron transfer from the excited pyrene fluorophore to the gold nanoparticles. A similar deactivation pathway may be responsible for the further decrease of its luminescence intensity after the formation of CNT–Au nanoparticle composites. This simple strategy for the high-density assembly of gold nanoparticles onto the surface of carbon nanotubes has been applied to other linking molecules such as *N*-(1-naphthyl)ethylenediamine and phenethylamine, demonstrating that molecules with similar structures can also serve as effective interlinkers. The CNT–Au nanoparticle composites may be conceived for applications in CO oxidation and other catalytic reactions. This approach to assembling

spherical gold nanoparticles may also be extended to form CNT–Au nanorod heterojunctions for electronic connection and molecular sensing.

Acknowledgment. This work was supported by a grant from the National Science Council of Taiwan (NSC 93-2113-M-007-034).

Supporting Information Available: High-resolution TEM image of the CNT–Au nanoparticle composites. This material is available free of charge via the Internet at <http://pubs.acs.org>.

References and Notes

- (1) Lordi, V.; Yao, N.; Wei, J. *Chem. Mater.* **2001**, *13*, 733.
- (2) Yu, R.; Chen, L.; Liu, Q.; Lin, J.; Tan, K.-L.; Ng, S. C.; Chan, H. S. O.; Xu, G.-Q.; Hor, T. S. A. *Chem. Mater.* **1998**, *10*, 718.
- (3) Han, L.; Wu, W.; Kirk, F. L.; Luo, J.; Maye, M. M.; Kariuki, N. N.; Lin, Y.; Wang, C.; Zhong, C.-J. *Langmuir* **2004**, *20*, 6019.
- (4) Satishkumar, B. C.; Vogl, E. M.; Govindaraj, A.; Rao, C. N. R. *J. Phys. D: Appl. Phys.* **1996**, *29*, 3173.
- (5) Ramanathan, T.; Fisher, F. T.; Ruoff, R. S.; Brinson, L. C. *Chem. Mater.* **2005**, *17*, 1290.
- (6) Jiang, K.; Eitan, A.; Schadler, L. S.; Ajayan, P. M.; Siegel, R. W.; Grobert, N.; Mayne, M.; Reyes-Reyes, M.; Terrones, H.; Terrones, M. *Nano Lett.* **2003**, *3*, 275.
- (7) Kim, B.; Sigmund, W. M. *Langmuir* **2004**, *20*, 8239.
- (8) Correa-Duarte, M. A.; Sobal, N.; Liz-Marzán, L. M.; Giersig, M. *Adv. Mater.* **2004**, *16*, 2179.
- (9) Correa-Duarte, M. A.; Pérez-Juste, J.; Sánchez-Iglesias, A.; Giersig, M.; Liz-Marzán, L. M. *Angew. Chem. Int. Ed.* **2005**, *44*, 4375.
- (10) Mieszawska, A. J.; Jalilian, R.; Sumanasekera, G. U.; Zamborini, F. P. *J. Am. Chem. Soc.* **2005**, *127*, 10822.
- (11) Chen, R. J.; Zhang, Y.; Wang, D.; Dai, H. *J. Am. Chem. Soc.* **2001**, *123*, 3838.
- (12) Artyukhin, A. B.; Bakajin, O.; Stroeve, P.; Noy, A. *Langmuir* **2004**, *20*, 1442.
- (13) Taft, B. J.; Lazarek, A. D.; Withey, G. D.; Yin, A.; Xu, J. M.; Kelley, S. O. *J. Am. Chem. Soc.* **2004**, *126*, 12750.
- (14) Georgakilas, V.; Tzitzios, V.; Gournis, D.; Petridis, D. *Chem. Mater.* **2005**, *17*, 1613.
- (15) Liu, L.; Wang, T.; Li, J.; Guo, Z.-X.; Dai, L.; Zhang, D.; Zhu, D. *Chem. Phys. Lett.* **2003**, *367*, 747.
- (16) Thomas, K. G.; Kamat, P. V. *J. Am. Chem. Soc.* **2000**, *122*, 2655.
- (17) Kuo, C.-H.; Chiang, T.-F.; Chen, L.-J.; Huang, M. H. *Langmuir* **2004**, *20*, 7820.
- (18) Kim, N. S.; Lee, Y. T.; Park, J.; Ryu, H.; Lee, H. J.; Choi, S. Y.; Choo, J. *J. Phys. Chem. B* **2002**, *106*, 9286.
- (19) Ipe, B. I.; Thomas, K. G. *J. Phys. Chem. B* **2004**, *108*, 13265.
- (20) Guarise, C.; Pasquato, L.; Scrimin, P. *Langmuir* **2005**, *21*, 5537.
- (21) Thomas, K. G.; Barazzouk, S.; Ipe, B. I.; Joseph, S. T. S.; Kamat, P. V. *J. Phys. Chem. B* **2004**, *108*, 13066.
- (22) (a) Kalyanasundaram, K.; Thomas, J. K. *J. Am. Chem. Soc.* **1977**, *99*, 2039. (b) Huang, M. H.; Dunn, B. S.; Zink, J. I. *J. Am. Chem. Soc.* **2000**, *122*, 3739.
- (23) (a) Makarova, O. V.; Ostafin, A. E.; Miyoshi, H.; Norris, J. R., Jr.; Meisel, D. *J. Phys. Chem. B* **1999**, *103*, 9080. (b) Rossetti, R.; Brus, L. E. *J. Chem. Phys.* **1982**, *76*, 1146.
- (24) Avouris, P.; Persson, B. N. J. *J. Phys. Chem.* **1984**, *88*, 837.